Development of an Improved Performance Function for the Control of Flow Separation

Brandon M. Reese*, Farrukh S. Alvi†, and Emmanuel G. Collins Jr.‡

Florida Center for Advanced Aero-Propulsion

Florida A&M University - Florida State University

Tallahassee, FL, 32310, USA

Feedback control of aerodynamic flow separation is a formidable challenge due to the nonlinear system dynamics and the lack of a closed-form model that describes these dynamics. Recently, adaptive control approaches have been employed to meet this challenge. However, the performance and robustness achieved using these algorithms is limited due to the fact that the sensors in flow control systems are not used to estimate lift and drag, the quantities of interest. This paper derives a physics-based performance function that is based on estimating the ratio lift/drag and correlates closely with simulated and experimental aerodynamic performance. The developments are based on a NACA 0025 airfoil at a range of near-transitional Reynolds numbers and a range of pre-stall and post-stall angles of attack. The simulation and experimental results consider the use of four pressure measurements. Both the simulated and experimental results indicate that the resulting performance function has properties favorable to closed-loop control. The performance function developed here may be applied to any feedback control framework.

*Graduate Research Assistant, Department of Mechanical Engineering, bmr09f@my.fsu.edu.

†Professor and FCAAP Director, Department of Mechanical Engineering, alvi@eng.fsu.edu, Associate Fellow AIAA.

‡Professor and Chair, Department of Mechanical Engineering, ecollins@eng.fsu.edu.

Nomenclature

Flow and Geometry Variables

α	Angle of attack (between chord and freestream)
α_{sep}	Angle of attack at separation
θ	Local angle between surface normal and freestream
θ_i	Local angle between surface normal and chord at sensor i
ρ	Air density
b	Airfoil span
c	Chord length
C_L	Lift coefficient
C_D	Drag coefficient
D	Drag
L	Lift
L_{max}	Maximum potential flow lift over all transitional Reynolds numbers
p	Static pressure
p_i	Static pressure at transducer i
P_{rms}	Unsteady pressure
$\frac{\partial p}{\partial x}$	Slope of pressure with respect to chord dimension
Re	Reynolds number based on chord length
U_∞	Freestream velocity
V_{lift}	Lift-based performance function
w_i	Trapezoidal summation weights
Z_{lift}	Lift-approximating function

I. Introduction

Several areas of flow control research, including suppression of cavity flow resonant tones and mitigation of flow separation, have advanced rapidly in recent years as new technologies have both created demand for and expanded the capabilities of such systems. The study of cavity flow control has demonstrated that mathematical techniques such as Proper Orthogonal Decomposition (POD) and model reduction are effective tools for developing control design models for aerodynamic systems, and the resulting models have also been applied to perform flow separation control.[1,2,3] While these studies incorporated flow visualization and analysis efforts to produce nonlinear models that are effective for developing open-loop control strategies, it has been impractical to apply these methods in closed-loop control.[4,5]

This research examines the problem of mitigating aerodynamic flow separation, which is of great interest in many areas such as aircraft wings, design of efficient turbine and compressor blades, and rotary wing flight. The phenomenon of flow separation is caused in a cumulative fashion by a sufficiently large negative pressure gradient on an aerodynamic boundary. Such negative pressure gradients are usually the result of flow over surfaces with convex curves or edges. Separation of the boundary layer results in flow recirculation in the separated region and therefore causes both decreased lift and increased drag on an airfoil as well as unsteadiness, which is also undesirable.

Although many open loop control systems have been examined, relatively few closed-loop separation control systems have been studied and successfully implemented.[6] Feedback control of aerodynamic flow separation is a formidable challenge due to the nonlinear system dynamics and the lack of a closed-form model that describes these dynamics. These difficulties have motivated the use of adaptive control approaches. The recent work by Tian et al. (2006) is the first to incorporate a sophisticated adaptive control approach, in particular ARMARKOV online system identification and the ARMARKOV adaptive disturbance rejection algorithm. That research, however, only presents results for stationary systems and very limited flow parameters: only one Reynolds number and one fixed angle of attack. In order to perform optimally, the algorithm presented would theoretically require unique tuning at each combination of angle of attack and Reynolds number. More recent work[7] presents performance for multiple angles of attack but does not take advantage of the multiple pressure measurements available on the experimental platform.

The study presented in this paper develops a performance function that enables efficient use of an

arbitrary number of pressure sensors and can handle a wide range of Reynolds numbers and angles of attack. This performance function is applicable to any feedback control approach, including the adaptive approach used by Tian et al.

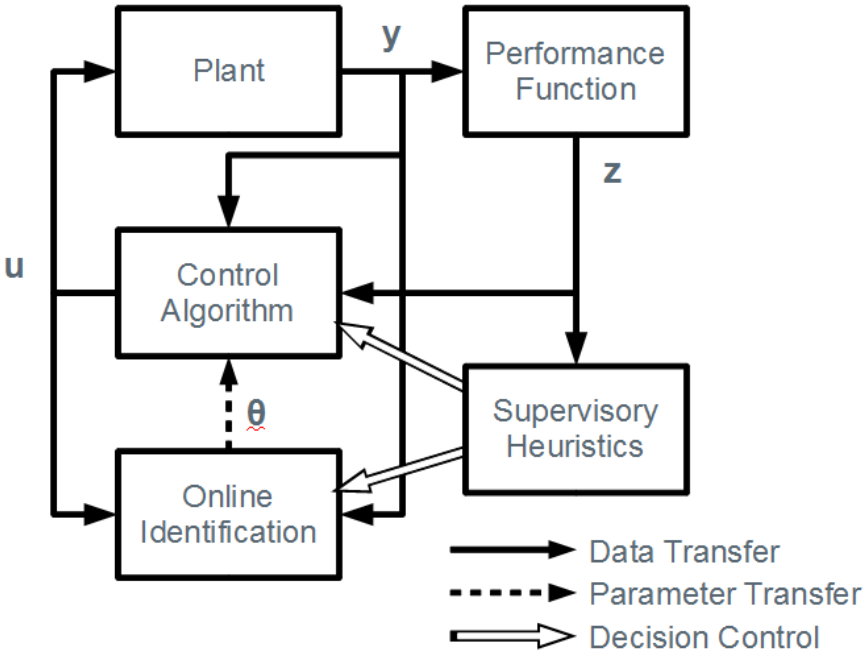

Figure 1. Adaptive Control Block Diagram

The adaptive control system of Fig. 1 operates based on an online identification algorithm and modular control block that could represent one of many control algorithms. The supervisory heuristics enable or disable the control, identification, and optimization segments of the adaptive algorithms based on the logic presented by Sane et al.[8] In the original formulation, a gradient descent algorithm updates the controller parameters in a way that reduces the cost function at each control iteration assuming that the identified system is approximately constant over the past n time steps, where n is the order of the identified system model. As the algorithm converges, the controller and online identification find an actuation scheme using multiple arrays of microjets that minimizes the specified cost function. System identification takes place at the same time as control updates.

The aim of this research is to maximize lift via closed-loop control, thereby mitigating boundary layer separation, in a manner that is effective for dynamically pitching angles of attack and a range of incoming flow speeds. The control system to accomplish this task will consist of online system identification of a linear, time-varying model and an adaptive controller. This paper shall present the algorithms used as well as the derivation of a performance function that projects sensor measurements to detect the rate of change of the desired physical quantity, namely the aerodynamic lift coefficient.

This paper is organized as follows. Section II describes the derivation of the Lift-Based Performance Function, Section III presents simulation and experimental data by which the performance function is validated. Finally, Section IV provides a summary and potential applications for this performance function.

II. Formulation of Lift-Based Performance Function

Earlier approaches to adaptive flow separation control have passed one or more pressure transducers to the controller as elements of the system output vector y and select a single transducer signal as the controller's performance signal z.[6] However, often it is desirable to define a scalar performance function using more than one sensor. Unfortunately, due to the complexity of fluid dynamics, it is not obvious how each sensor contributes to the performance function. Rather than minimizing the pressure fluctuation at some selected sensor, this paper seeks to minimize a physics-based performance variable that incorporates

the pressure signals from all sensors. To do this, it is necessary to approximate the aerodynamic pressure force vector based on a set of pressure transducer measurements.

For typical aerodynamic applications, an airfoil's efficiency is measured by the lift-to-drag ratio L/D that is achieved during operation. Ideally, this research aims to develop a performance function that may be used to optimize L/D, allowing for dynamic flow conditions that are unknown *a priori*. To perform optimal control of separation over an airfoil, it is desirable to attain a performance function that has its minimum where L/D, or equivalently the ratio of normalized quantities C_L/C_D, is optimized. Additionally, this mininmum should be unique in parameter space in order to avoid convergence to a local minimum. The equations that describe the pressure contribution to the lift and drag coefficients,

$$C_L = \frac{2 \oint p \sin(\theta) dA}{\rho {U_\infty}^2 bc} \tag{1}$$

and

$$C_D = \frac{2 \oint p \cos(\theta) dA}{\rho {U_\infty}^2 bc}, \tag{2}$$

involve pressure integrals over the airfoil surface, which are not directly evaluated in experiments because the integral requires unrealistic sensor resolution. Let θ, illustrated in Fig. 2, represent the angle between the airfoil's local surface normal and the free stream velocity. Useful normalization to to the lift and drag coefficients is achieved by dividing the force quantities by a characteristic force quantity, $\frac{1}{2}\rho {U_\infty}^2 bc$, where ρ is the flow density, U_∞ is the free stream velocity, b is the span, and c is the chord length. As long as we can show that the pressure distribution being integrated is well-behaved, it is more practical to approximate these integrals with their corresponding summations using a discrete number of sensors. This approximation is the basis of the lift-based performance function presented in this paper.

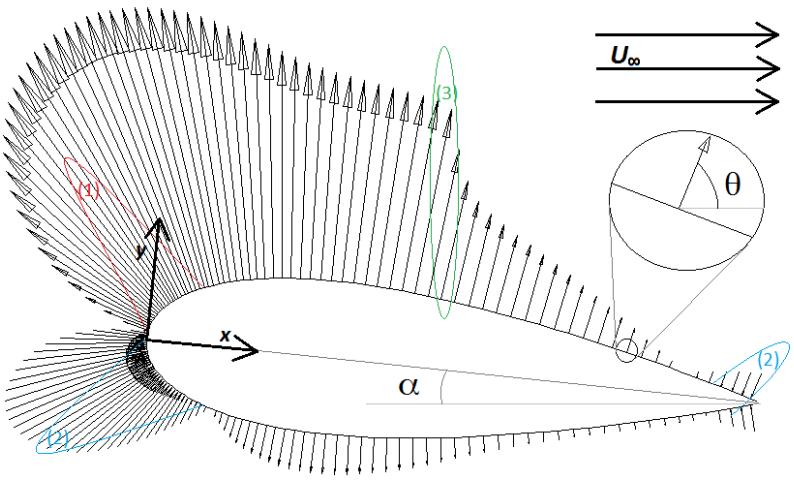

Figure 2. XFOIL Simulation of NACA 0025, 6 degrees, Re = 100,000

Figure 2 is a pressure distribution for turbulent flow that was obtained computationally using a numerical panel method that accounts for viscosity for the transitional range Reynolds number 10^5. The simulation assumed incompressible flow and thus applied low Mach number flow dynamics. By physical intuition, one observes three features of the pressure distribution, labeled in Fig. 2: (1) negative pressure gradient due to the acceleration caused by the impeded flow, (2) locally maximum positive pressure locations corresponding to the two stagnation points (fore and aft), and (3) apparent discontinuity on the top surface, indicating early stages of flow separation at the rear of the airfoil. Inspecting this and many other pressure distribution plots has led to some key observations. First, the surface pressure will never exceed the free stream stagnation pressure; this bounds the pressure distribution from above. Additionally, the surface pressure will be bounded from below by the solution of the potential flow (inviscid case, $Re \to \infty$), which can be solved analytically by using a conformal mapping. Lastly, the gradient $\frac{\partial p}{\partial x}$ is bounded as long as we consider incompressible

Mach numbers (no shocks). Furthermore, the separation point and the high turning angles at the leading edge produce the largest gradients along the chord.

As a result of these observations, it is hypothesized that a limited number of discrete pressure measurements can be used to compute an approximation of aerodynamic forces that is sufficiently accurate to use as a control feedback variable. The aerodynamic pressure force is by definition a path integral of the pressure normal vectors around the surface of the airfoil. As described in Eqs. (1) and (2), this vector can be decomposed into two components: lift, which is normal to the free stream, and drag, which is parallel to the free stream. Note that this is only one of the components comprising the total drag force since shear force must also be accounted for. It is assumed that pressure data alone will provide a sufficient estimation for separation control purposes. This assumption is justified by the data presented in Appendix A, which indicates that points of maximal lift and points of maximal L/D are coincident for transitional Reynolds numbers.

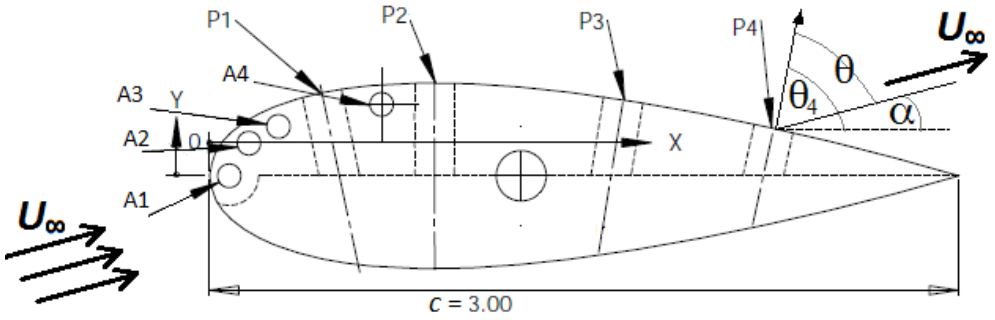

Figure 3. Airfoil Microjet Array and Pressure Transducer Schematic

An approximation of lift that is suitable for control purposes must practically preserve the global maximum of the actual lift quantity. The design of Fig. 3 is based on the hypothesis that four pressure sensors (marked P1 through P4) provide sufficient resolution to preserve the global maximum. An additional desired trait of a lift-based performance function is that the function is positive definite about the optimal (design) point in flow condition space and that in its time derivative, it satisfies the negative definite condition of a Lyapunov function. This behavior is important because it permits control of a nonlinear system to converge to the optimal point while operating over a range of conditions.

Proposed here is a performance function along with validating results from both simulation and experimental data. Using four pressure sensors located along the airfoil center chord, a lift approximation is obtained in the following manner: take a weighted average of the calibrated pressure signals using $\sin(\theta)$ at each transducer location as a weighting function. Note that θ, the normal angle relative to the freestream, depends on both airfoil geometry and angle of attack. For this formulation, we assume that airfoil geometry angle (denoted θ_i relative to the chord axis) is known but angle of attack (α) is unknown, as this parameter would change during typical operation. The sine function in the lift integral (1) has argument $\theta = \theta_i - \alpha$. We assume a constant value for α, which introduces a tolerable error to the summation weights. Since flow separation is the phenomenon to be controlled, the $11.5\,^\circ$ average separation angle (α_{sep}) for the NACA 0025 is a reasonable choice for the constant angle of attack parameter. For the range of angles of attack considered in this study ($\alpha \in [0\,^\circ\ 16\,^\circ]$) the error induced may be evaluated directly by comparing $\sin(\theta_i - \alpha)$ with $\sin(\theta_i - \alpha_{sep})$ for each of the four sensors. This calculation has been performed and in Fig. 4 is expressed as percent error for the computed weight of each sensor.

For the assumed range of flight conditions, Fig. 4 reveals we may ignore variations in the angle of attack when evaluating these weights with a penalty in accuracy of less than 7%. More importantly, the airfoil geometry component, which is known *a priori*, captures what an intuitive physical understanding of the problem would suggest: pressure sensors toward the leading edge, which are more vertically oriented, will provide more information about lift and less information about drag. Conversely, the rear sensors have a greater lateral component and therefore give a better indication of pressure drag than do their upstream counterparts. When evaluating the performance function, only the lift approximation is used because the drag approximation is subject to higher uncertainty and the changes in the lift coefficient alone are a good indicator of separation effects. Although only lift is accounted for in the design of the performance function, comparisons to the full L/D quantity have been made in validation, and the performance function

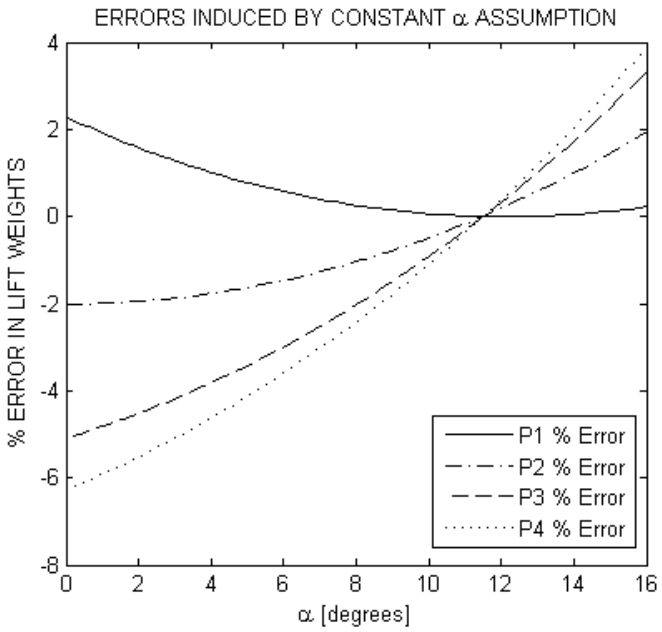

Figure 4. Percent errors when angle approximation $\alpha = \alpha_{sep}$ is used

approximates the shapes of these curves adequately well (see plots in the Appendix). XFOIL simulation results confirm that there is little to no difference in the optimal lift point and the optimal L/D point in each angle of attack series. The Lift-Approximating Function, Z_{lift}, and the Lift-Based Performance Function, V_{lift}, may be computed as

$$Z_{lift} = \sum_{i=1}^{N} w_i \sin(\theta_i - \alpha_{sep}) p_i, \tag{3}$$

$$V_{lift} = (L_{max} - Z_{lift})^2, \tag{4}$$

where weights w_i appear in the summation to approximate the integral using N trapezoidal regions based on the pressures measured at each sensor p_i.

III. Results

The results of the XFOIL analysis as well as some experimental validation are presented in this section. The XFOIL program solves viscous flow around an airfoil using an iterative panel method and turbulence modeling. The program is mainly used for optimal airfoil design because it produces high-fidelity lift and drag predictions. Experimental data has also been used to further validate the analytically derived performance function.

A. Simulation Results

To evaluate the performance function in simulation, XFOIL viscous simulations have been run for each combination of *eleven Reynolds numbers* and *each integer angle of attack* from 0° to 16°. From these simulations, the 4 surface pressure values at the respective pressure transducer locations were the only information extracted from the simulation used to compute V_{lift}.

Figures 5, 6, and 7 present the evaluated performance function on the vertical axis and shifted angle of attack on the horizontal axis. The angle of attack is shifted to represent the difference, in degrees, from the point of maximum L/D ratio. (These optimal angles come from L/D peaks in plots such as in Fig 8.) Ideally, every curve should have it's minimum at $\alpha - \alpha_{optimal} = 0$, and for the transitional Reynolds numbers (80,000 through 120,000), this is the case. From the simulation data it can be seen that this behavior breaks

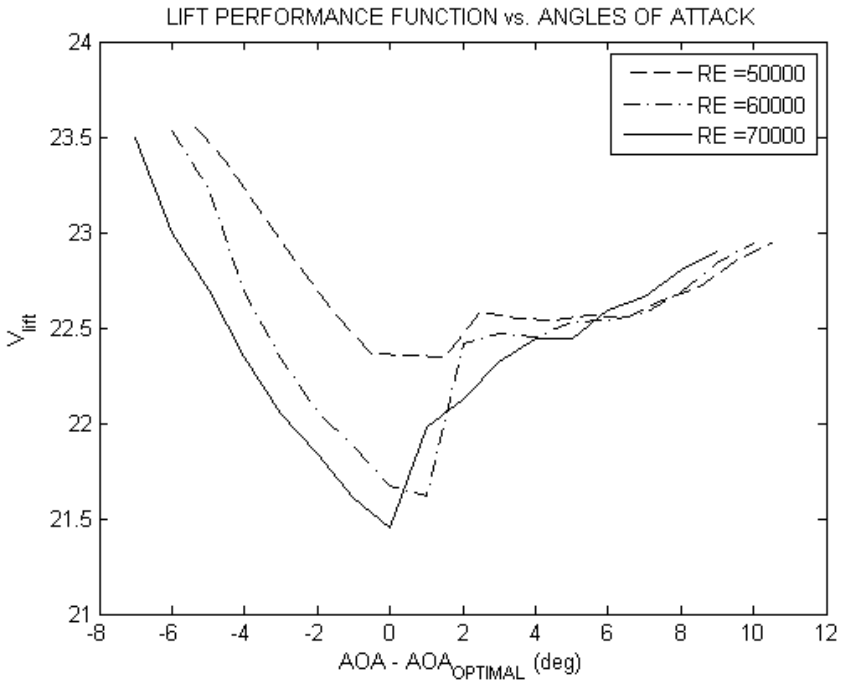

Figure 5. V_{lift} **for lower Reynolds numbers, evaluated from simualated pressures**

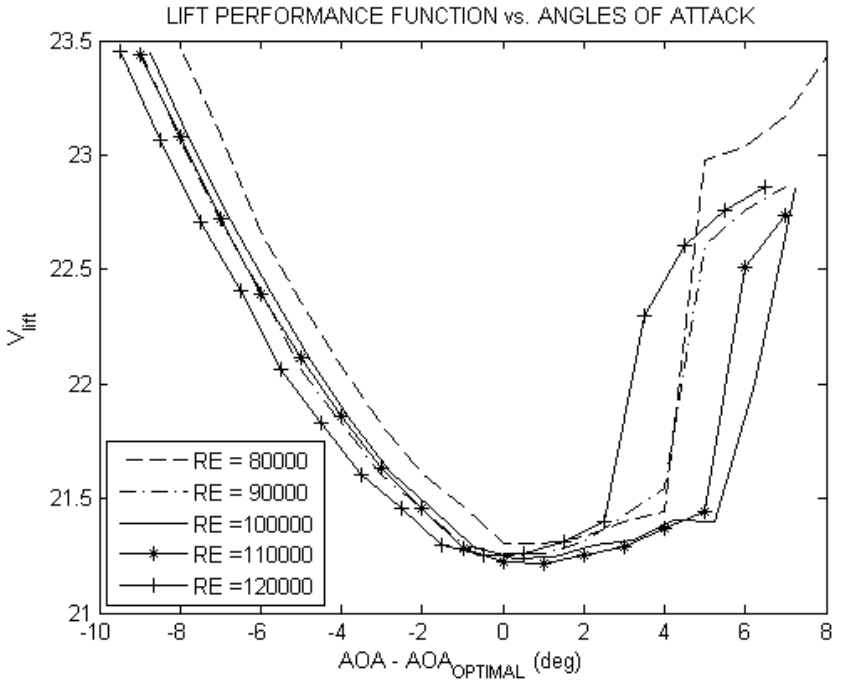

Figure 6. V_{lift} **for transitional Reynolds numbers, evaluated from simualated pressures**

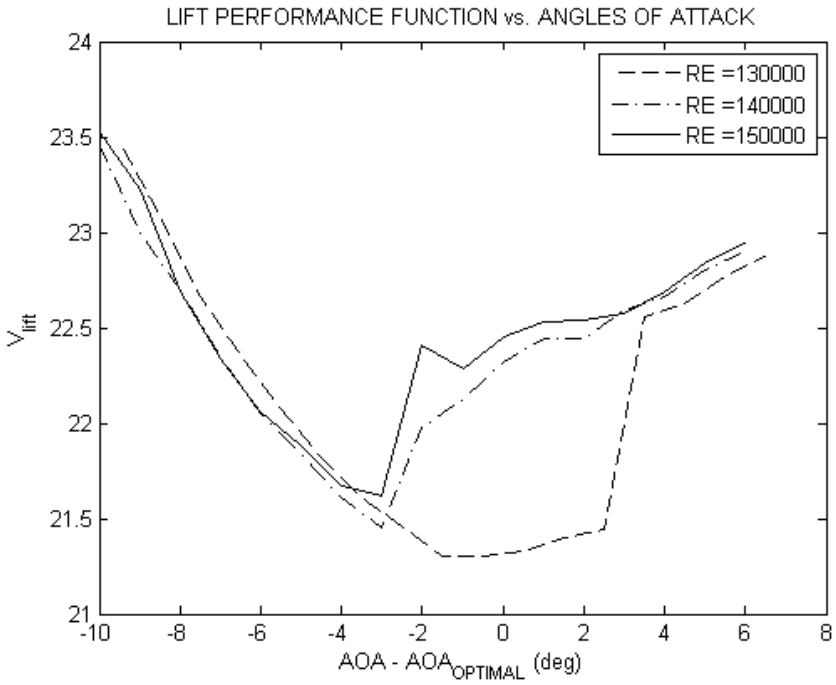

Figure 7. V_{lift} **for higher Reynolds numbers, evaluated from simualated pressures**

down for Reynolds numbers outside of this range; however, it should be noted that for the higher Reynolds number off-design cases, V_{lift} tends to behave conservatively, favoring lower angles of attack. This means that even for Reynolds numbers outside of the transitional range, the control system, although giving up some optimality due to conservatism, should drive the system to the attached region as opposed to the separated region.

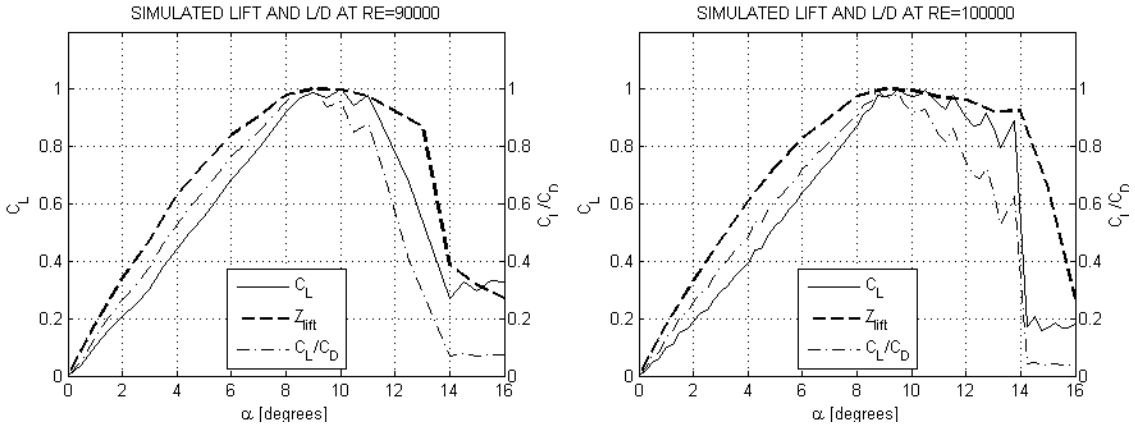

Figure 8. Lift Coefficient and L/D **for** $Re = 90000$ **and** $Re = 100000$

B. Experimental Results

Lift and drag force measurement tests were performed in a subsonic, closed return, wind tunnel with a 12" x 12" test section on a NACA 0025 airfoil. The wind tunnel velocity corresponds to a Reynolds number of 1.0×10^5. The airfoil is designed to be modular so that multiple arrays of microjets can be utilized as well as multiple arrays of pressure sensors. Multiple airfoils are built allowing for tests to be performed with and without the use of Endevco unsteady pressure transducers. The stationary angle of attack can be modified by

changing out the bottom cover of the airfoil. Currently, bottom covers have been manufactured for 0°, 2°, 4°, 6°, 8°, 9°, 10°, 11°, 12°, 13°, 14°, 15°, 16°, 18°, 20°, and 22°; therefore, up to this point force measurements using this configuration are attainable only at this resolution. These angles were selected to allow lift and drag readings to be recorded over a large span of angles, while allowing for a better understanding of baseline flow as well as a higher level of accuracy in determining where flow is separating. It is assumed that flow will separate around $11° - 12°$ angle of attack.

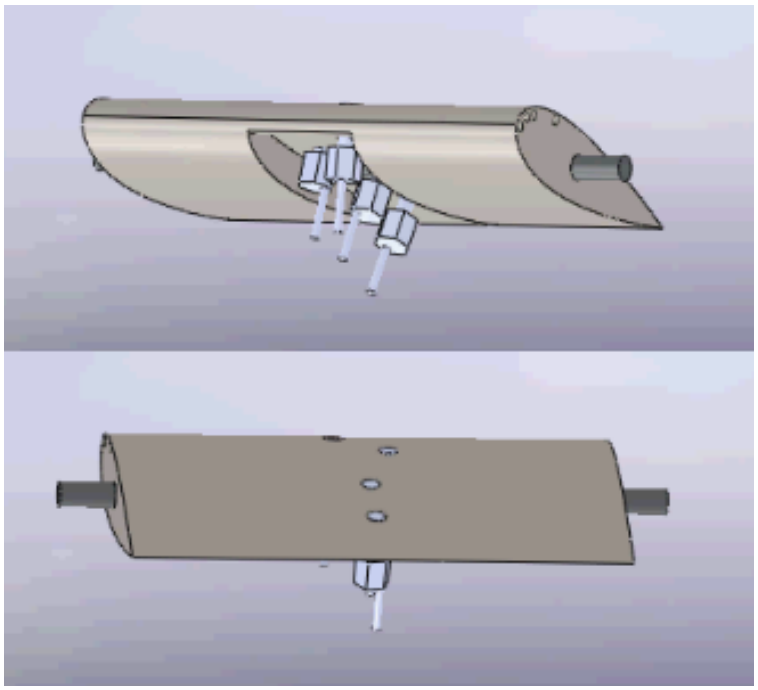

Figure 9. Assembled Airfoil CAD with Pressure Transducers

Lift tests were completed in this experimental configuration, and for comparison purposes, pressure transducers were installed on a separate NACA 0025 airfoil in each of the four design locations (p1-p4 location shown in Fig. 3). A CAD illustration of the tunnel model with installed pressure transducers is given in Fig. 9. After calibrating the pressure transducers, the experimental pressure signals were given as inputs to the same function for Z_{lift} that was used in the simulation tests. Figure 10 shows the lift measurements compared with the performance function evaluated for three trials of experimental data. In this experiment, total flow separation occured between 14° and 15°. The predictions made by the lift performance function match very well when compared to the measured lift values, capturing the over trend of increasing lift and the drop caused by the separation event. For the sake of comparison, the p_{rms} plot for a single sensor is given in Fig. 11 (p_4 gave the best results for this Reynolds number). Although this more traditional performance function distinguishes between separated and attached regimes, the presence of local maxima may lead to convergence to a local minimum of L/D.

Ideally, the experimental data plot (Re of approximately 95,000) should closely match the shape of the simulated data plots of Fig. 8. The difference between simulation and laboratory results is primarily due to the unpredictable nature of the transition in the boundary layer from laminar to turbulent flow. While the simulation evaluates the flow based on a turbulence model, the precise location at which a particular flow will transition is highly sensitive to surface roughness and is difficult to predict. In addition to the transition point uncertainty, the wind tunnel fan apparatus introduces turbulence that has not been accounted for in the simulated data. For this reason, the Reynolds number of the tunnel experiment is effectively higher than the computed value 95,000. The separation location observed in experiment is closer to the angle observed in the Re=110,000 simulation than either of the Re=90,000 or Re=100,000 simulations. Even though these difficulties exist in matching experimental flow separation to simulated flow separation, the performance function, based only on steady pressures, is able to make good estimates for both sets of data.

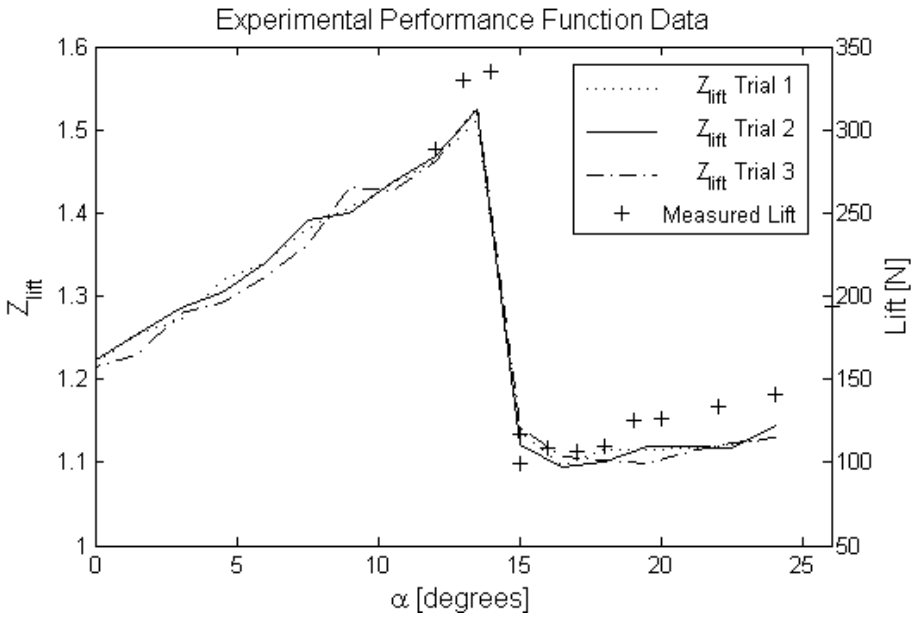

Figure 10. Z_{lift} **evaluated with measured pressures compared to measured lift for Re**$= 95,000$

IV. Conclusions and Future Work

The Lift-Based Performance Function, which is derived analytically and presented in this paper, is shown to (1) satisfy desired conditions of unique-minimum, monotonic, positive definite behavior surrounding optimal points for a wide range of flow conditions and (2) match physics in both experimental tests and widely-used simulation codes. While earlier adaptive control schemes for flow separation control have tried to minimize nonphysical performance functions based on pressure fluctuations at a single transducer location, this new approach applies a weighting function that systematically makes use of all transducer signals to better approximate system performance. The formulation can be generalized to many other airfoils and flow geometries, and although the choice of a symmetric airfoil allows for a straightforward analytical derivation, a performance function of the same form may be applied with minimal tuning to asymmetric airfoils, ramps, and other vehicle surfaces.

Future work includes a closed-loop experimental implementation which requires the selection of an actuator. Actuator development has also been key to the recent advances in the field of flow separation control. Both synthetic jet unsteady actuators[6,7] and steady microjet actuators[9,10] have been effective in separation control experiments. Because of the advantage of high momentum capability with low power requirements,[11] microjets have been selected as the primary actuators for the upcoming research. Results in this paper are presented with respect to angle of attack and Reynolds number. Demonstration that the lift performance function predictions generalize to microjet-actuated flows is an important next step. Since the derivation makes no assumptions that are violated in a microjet-actuated flow, it is expected that the lift approximation results under microjet actuation will be comparable to those under angle of attack actuation. The estimation problem under angle of attack actuation, in fact, is made slightly more difficult by the unmeasured effects of rotation of the lift vector. These rotation effects do not influence the lift approximation when the flow is actuated instead by microjets.

The continuation of this research will employ the performance function in an adaptive control scheme. The efficient computation of a single performance variable will enable adaptive control algorithms to run much more quickly than they would if they were given an input vector consisting of several pressure signals. The control systems mentioned in this paper will be implemented in a wind tunnel experiment with the algorithms executing on real-time processor hardware. The lift-based performance function should provide the robustness needed to handle changing flow conditions, which would allow future control research to address the problem of dynamic stall, a major issue in current flow control research.

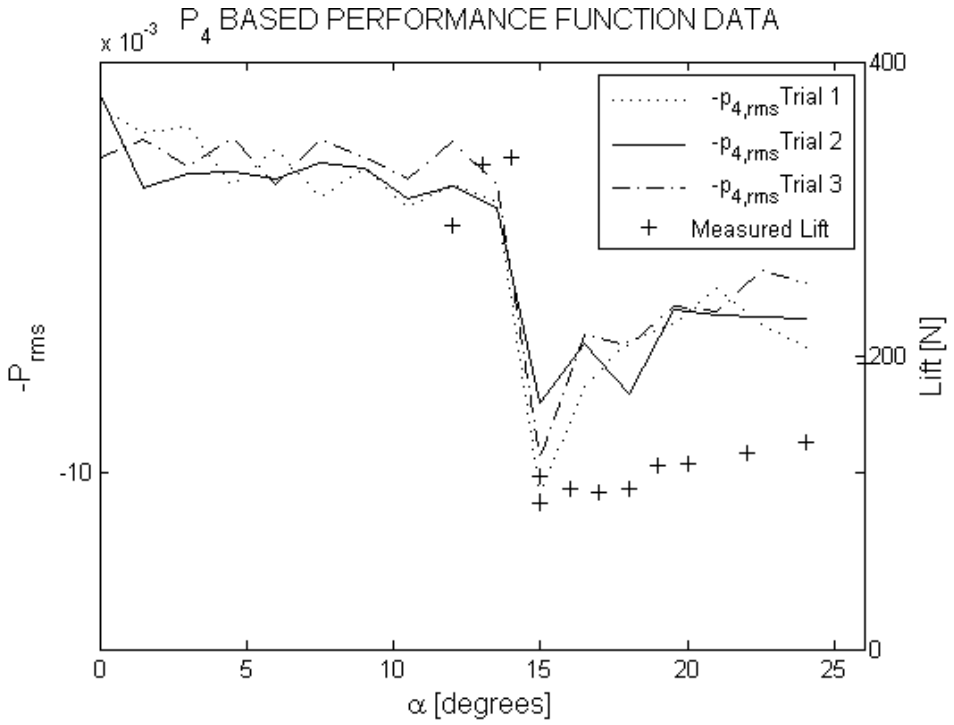

Figure 11. Measured lift and negative p_{rms} evaluated with a single measured pressure signal for Re=95,000

Appendix

A. Normalized Z_{lift}, C_L, and C_L/C_D vs α

These data points are from XFOIL viscous simulations. The lift approximating function Z_{lift} as well as C_L and C_L/C_D are dimensionless and normalized here for plotting purposes. Ideally, the maximum of each function should occur at the same angle of attack.

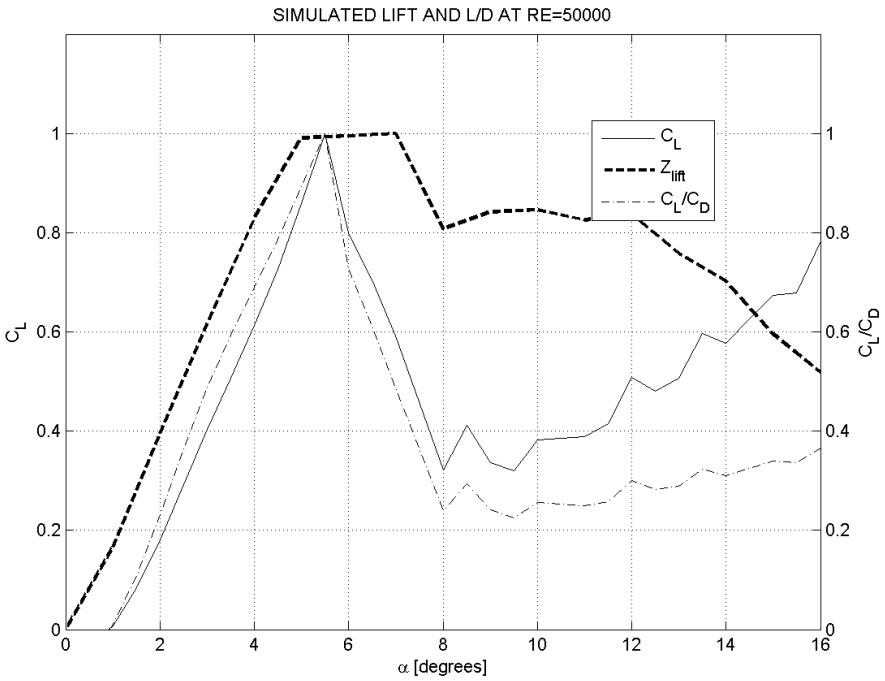

Figure 12. Lift Coefficient and L/D for $Re = 50000$

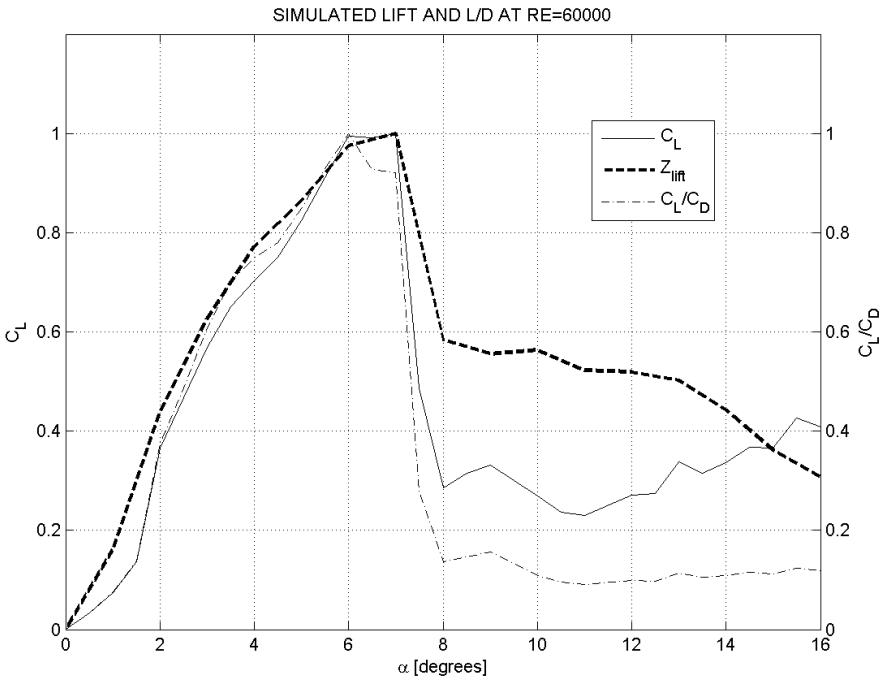

Figure 13. Lift Coefficient and L/D for $Re = 60000$

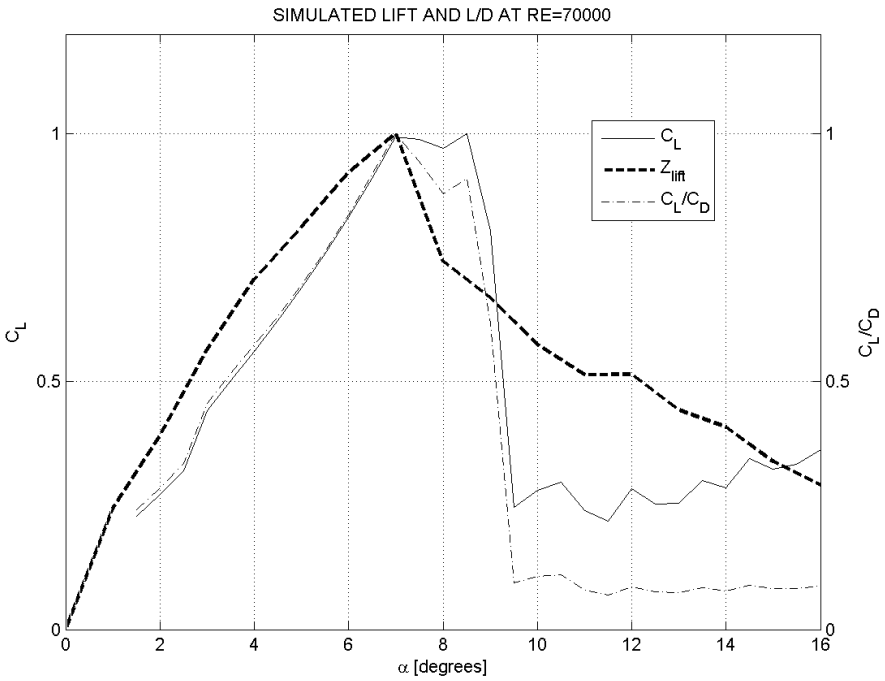

Figure 14. Lift Coefficient and L/D for $Re = 70000$

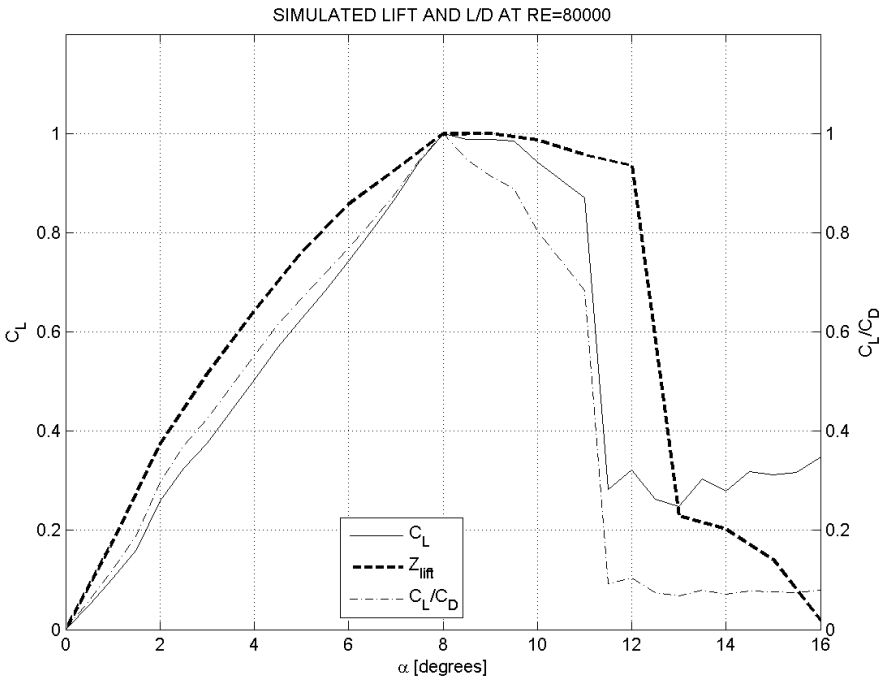

Figure 15. Lift Coefficient and L/D for $Re = 80000$

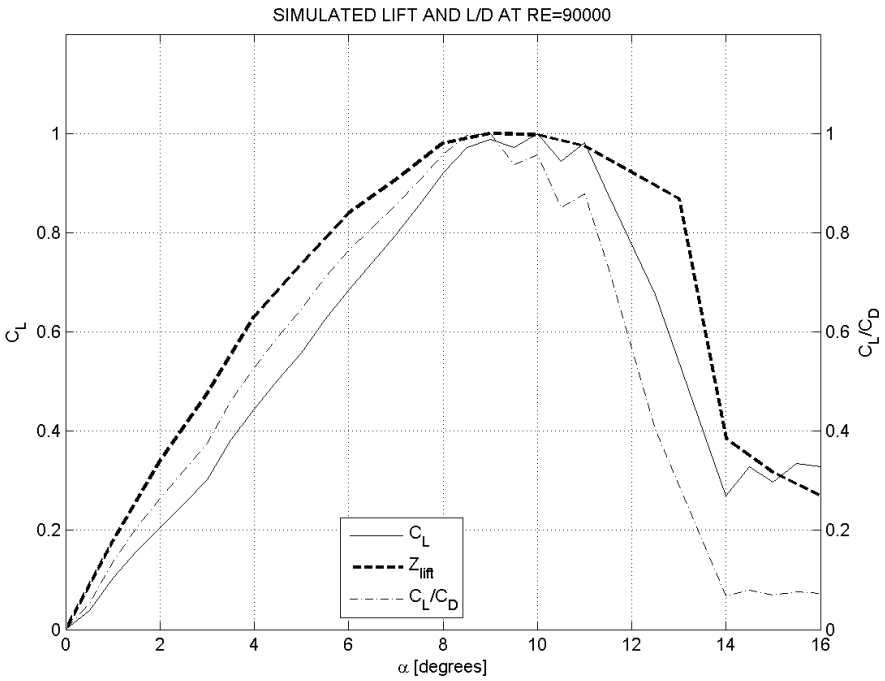

Figure 16. Lift Coefficient and L/D for $Re = 90000$

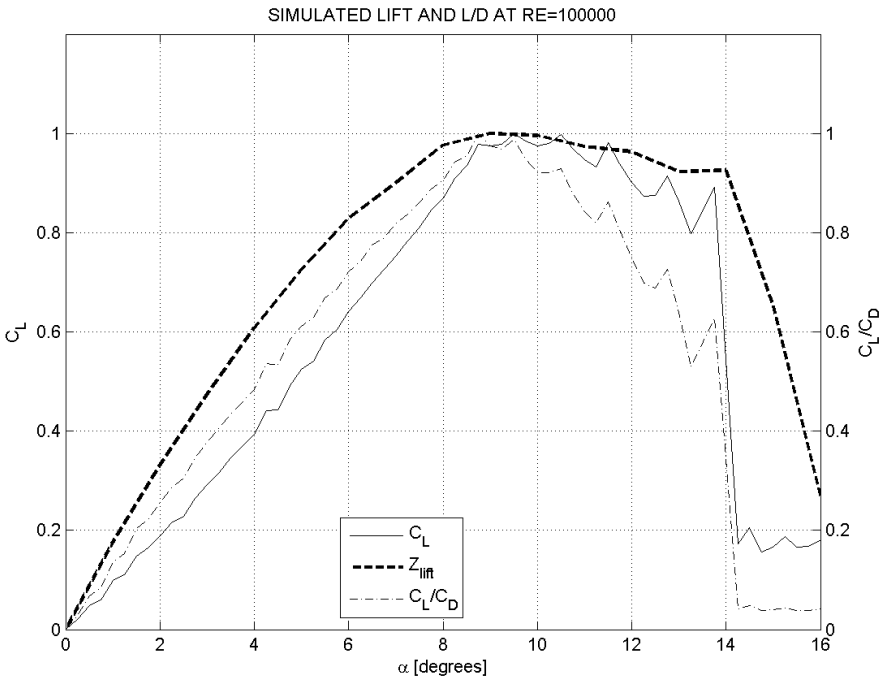

Figure 17. Lift Coefficient and L/D for $Re = 100000$

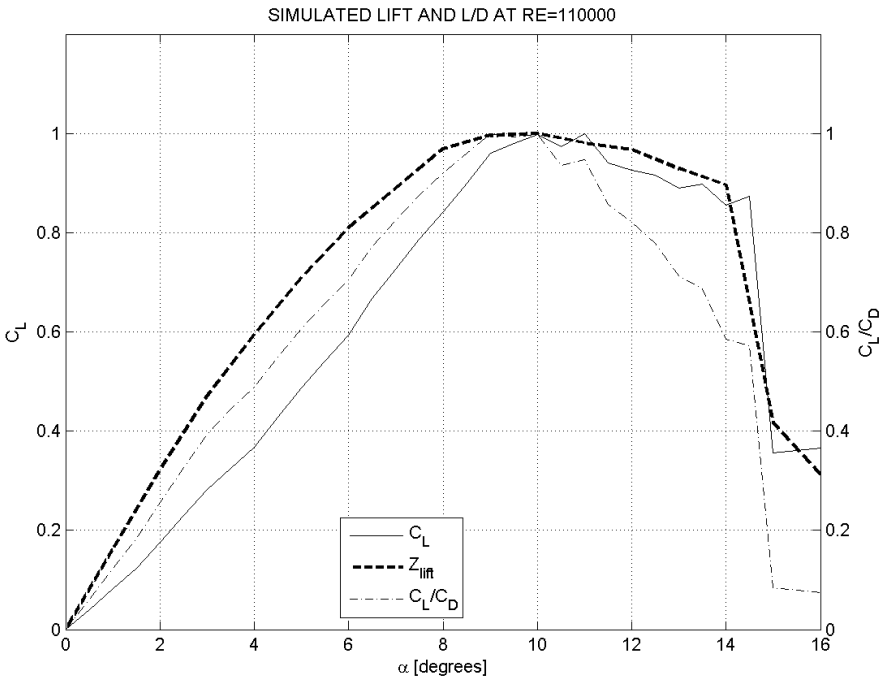

Figure 18. Lift Coefficient and L/D for $Re = 110000$

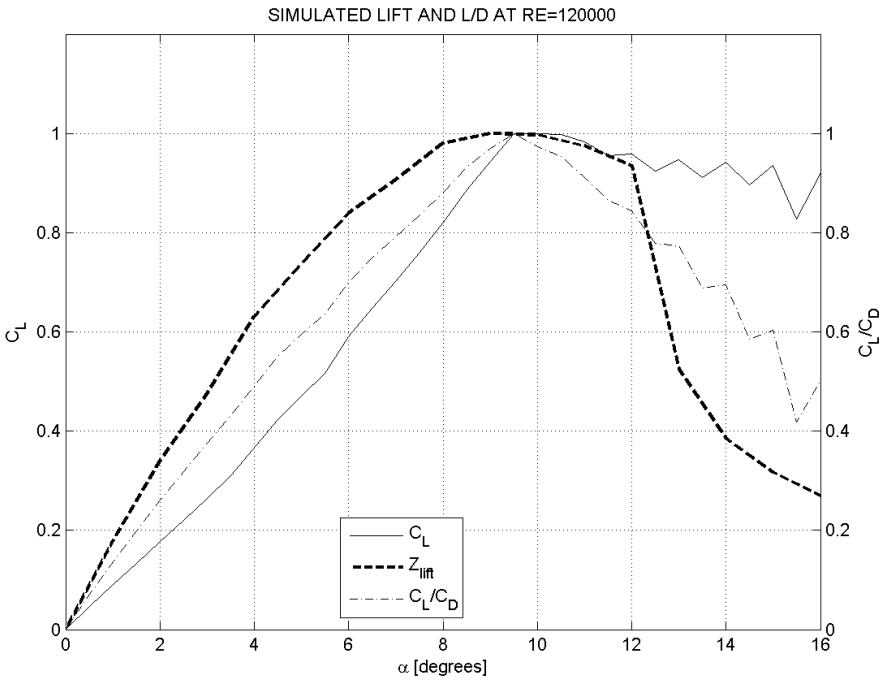

Figure 19. Lift Coefficient and L/D for $Re = 120000$

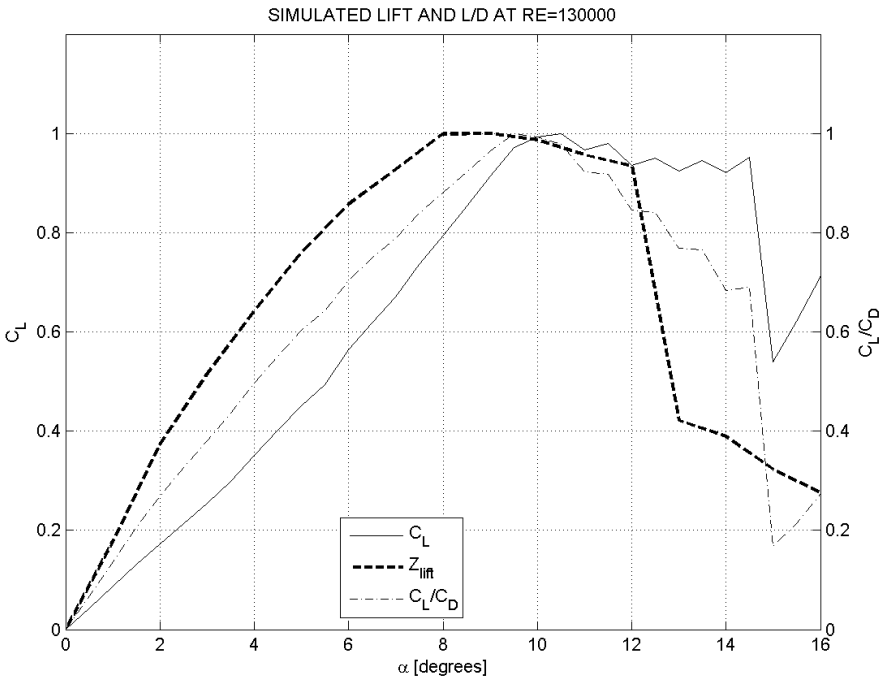

Figure 20. Lift Coefficient and L/D for $Re = 130000$

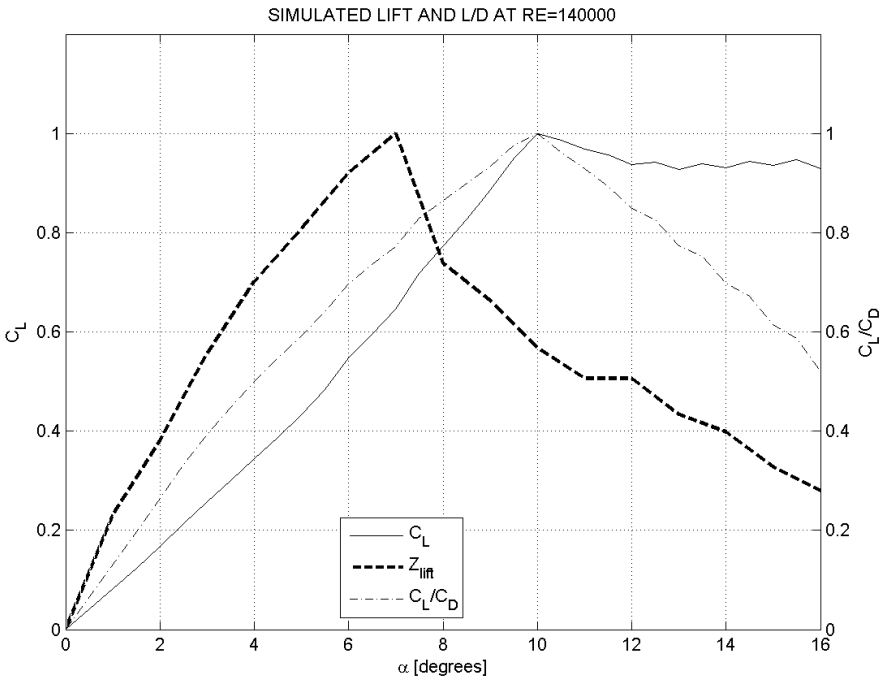

Figure 21. Lift Coefficient and L/D for $Re = 140000$

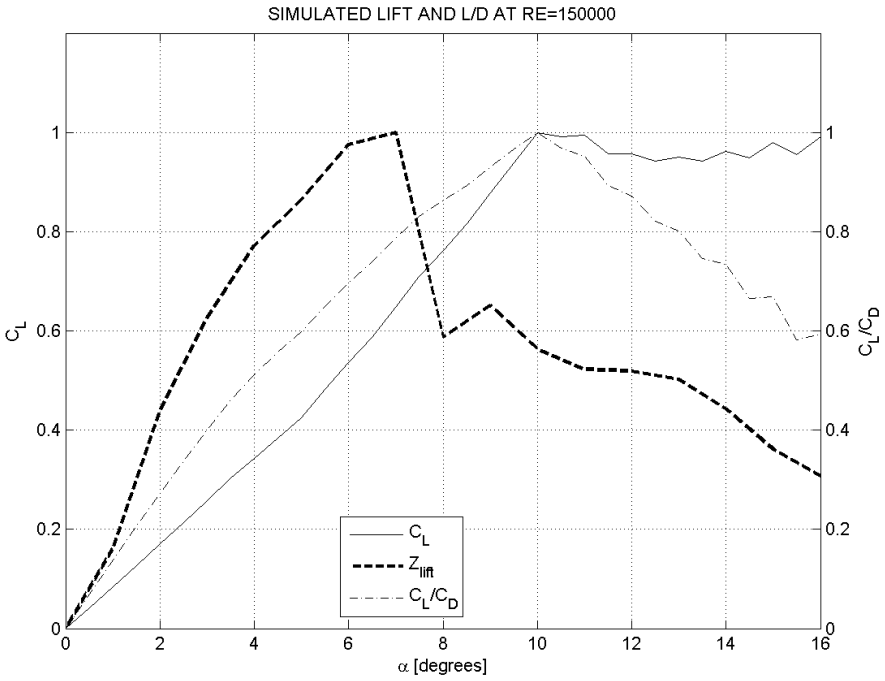

Figure 22. Lift Coefficient and L/D for $Re = 150000$

References

[1]M. Samimy, M. Debiasi, E. C. A. S. X. Y. J. L. J. M., "Feedback Control of Subsonic Cavity Flows Using Reduced-order Models," *Journal of Fluid Mechanics*, Vol. 579, 2007, pp. 315–346.

[2]E. Caraballo, J. Little, M. D. M. S., "Development and Implementation of an Experimental Based Reduced-order Model for Feedback Control of Subsonic Cavity Flows," *Journal of Fluids Engineering*, Vol. 129, No. 7, 2007, pp. 813–824.

[3]Favier, J., Kourta, A., and Leplat, G., "Control of Flow Separation of a Wing Profile using PIV Measurements and POD Analysis," *IUTAM Symposium on Flow Control with MEMS*, IMFT - French National Institute of Mechanics of Toulouse, IUTAM, Sept. 2006.

[4]P. Yan, M. Debiasi, X. Y. J. L. H. O. M. S., "Experimental Study of Linear Closed-loop Control of Subsonic Cavity Flow," *AIAA*, Vol. 44, No. 5, 2006, pp. 929–938.

[5]J. Little, M. Debiasi, E. C. M. S., "Effects of Open-loop and Closed-loop Control on Subsonic Cavity Flows," *Physics of Fuids*, Vol. 19, No. 065104, 2007.

[6]Tian, Y. and Cattafesta, L., "Adaptive Control of Flow Separation," *44th Aerospace Sciences Meeting and Exhibit*, Interdisciplinary Microsystems Group, AIAA, Reston, Va, Jan. 2006.

[7]Tian, Y., Song, Q., and Cattafesta, L., "Adaptive Feedback Control of Flow Separation," *3rd AIAA Flow Control Conference*, Interdisciplinary Microsystems Group, AIAA, Reston, VA, June 2006.

[8]Sane, H. S., Venugopal, R., and Bernstein, D. S., "Disturbance Rejection Using Self-Tuning ARMARKOV Adaptive Control with Simultaneous Identification," *IEEE Transactions on Control Systems Technology*, Vol. 9, IEEE, Jan. 2001, pp. 101–106.

[9]Chuy, O. Y., Kumar, V., Holt III, F. V., Collins Jr., E. G., and Alvi, F. S., "Microjet-based Separation Control Using a Virtual Sensor for Degree of Separation," *Florida Center for Advanced Aero-Propulsion Annual Technical Symposium*, FCAAP, Tallahassee, Fl, Aug. 2009.

[10]Alvi, F. S., "Adaptive Control of Inlet Separation Using Supersonic Microjets," Tech. rep., NASA Langley Research Center, Hampton, VA.

[11]Kumar, V. and Alvi, F. S., "Efficient Control of Separation Using Microjets," June 2005.